

Hong-bing Peng\*, Wei-qing Chen, Yan-chong Yu and Hong-guang Zheng

# Effect of Ultrasonic Melt Treatment on Solidification Structure of Fe-36Ni Invar Alloy

**Abstract:** The effect of ultrasonic treatment on the solidification structure of Fe-36Ni invar alloy was investigated. The experiment results showed that the ultrasonic treatment before its solidification had no significant effect on the solidification structure. However, when ultrasonic was inputted into the molten alloy during its solidification process, the primary dendrites were broken up into lots of fragments and solidification structure was refined significantly. When ultrasonic treatment was applied in the melt doped with yttrium before its solidification, ultrasonic cavitation could break up precipitates into many small ones, which could refine its solidification structure as nucleation cores. In samples containing yttrium treated by ultrasonic at 1753 K, the number of the precipitates was 623/mm<sup>2</sup> and its average size was 2.18  $\mu\text{m}$ ; while at 1803 K, they were 604/mm<sup>2</sup> and 2.34  $\mu\text{m}$  respectively. The ultrasonic cavitation had a similar effect at two different temperatures. The solidification structure refined greatly at 1753 K was due to its low pouring temperature.

**Keywords:** ultrasonic, Fe-36Ni, solidification structure, yttrium

**PACS® (2010).** 81.40.-z

**\*Corresponding author: Hong-bing Peng:** State Key Laboratory of Advanced Metallurgy, University of Science and Technology Beijing, Beijing 100083, China. E-mail: phbing1021@126.com

**Wei-qing Chen, Yan-chong Yu:** State Key Laboratory of Advanced Metallurgy, University of Science and Technology Beijing, Beijing 100083, China

**Hong-guang Zheng:** Technology Institute of Metallurgical, Baosteel Institute, Shanghai 201900, China

## 1 Introduction

Fe-36Ni alloy consists of an austenite-single phase structure and is notable for its uniquely low thermal expansion coefficient (TEC) under its Curie temperature. Not only has it been employed in temperature-independent instruments, such as precision measuring devices, but it has also served as special structure materials [1–3]. However, the continuous casting billets suffer serious cracking problems in hot rolling due to the lack of production expe-

rience and the immature production technology. And it can also be found that coarse grains in the billets have an adverse effect on the hot rolling while small ones can solve this problem to a certain extent, according to its continuous casting trial production. Ultrasonic treatment introduced into molten metal has a positive effect on grains refinement. In prior work, ultrasonic treatment applied in molten metal could create cavitation and acoustic streaming, causing the forming, growing, pulsating and collapsing of bubbles in molten metal [4, 5]. Lots of researches have investigated the effects of ultrasonic treatment on solidification structure and properties of metals [6–13]. Up to now, many investigations of ultrasonic on solidification processes have been focused on metals with a low melting point, only a few has been based on a high one. Therefore, the influence of ultrasonic on solidification structure of Fe-36Ni alloy is investigated. Meanwhile, the refining mechanism of ultrasonic treatment on solidification structure is discussed in detail.

## 2 Experimental procedures

### 2.1 Material and experimental apparatus

The chemical composition of Fe-36Ni invar alloy in the present study is shown in Table 1. And the melting point of the alloy is 1703 K. Fig. 1 shows the schematic illustration of experimental apparatus. The apparatus consists of carbon tube furnace, ultrasonic processing system, gas protection system and temperature control system. Ultrasonic generator is manufactured by Institute of Acoustics, Chinese Academy of Sciences. Its power and frequency are adjustable, range from 0 W to 300 W and 0 KHz to 100 KHz, respectively.

### 2.2 Experimental methods

Table 2 shows the detailed experimental process. Several groups of raw material were prepared in a carbon tube furnace. For groups 1–8 (G1–G8), about 500 g Fe-36Ni alloy was melted under flowing argon gas in an alumina

**Table 1:** Chemical composition of Fe-36Ni invar alloy (mass%)

C	Si	Mn	P	S	Cr	Al	Ni	Fe
0.013	0.17	0.29	0.008	0.001	0.12	0.007	36.22	Bal.

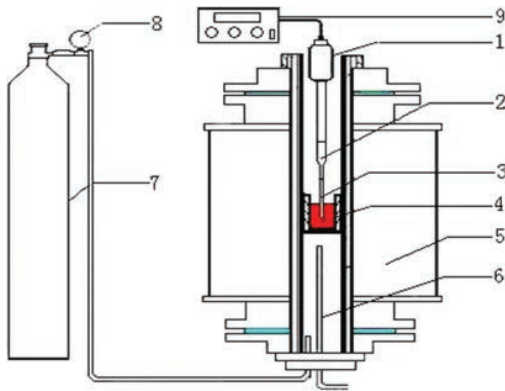


**Fig. 1:** Schematic illustration of experimental apparatus:  
 1 – ultrasonic transducer, 2 – ultrasonic amplitude transformer horn, 3 – probe, 4 – molten alloy (Fe-36Ni), 5 – carbon tube furnace, 6 – temperature control thermocouple, 7 – Ar gas, 8 – pressure gage, 9 – ultrasonic generator

crucible. After processing as described in Table 2, the melt was cooled in the furnace to room temperature or cast into an ingot mold and then air-cooled to room temperature. The temperature was measured with a B-type thermocouple and was controlled within  $\pm 5$  K of the treatment tem-

perature. A columnar ingot with a size of diameter 36 mm could be obtained.

Ultrasonic treatment was carried out based on the ultrasonic wave probe directly introduced into the molten alloy. The depth of the probe dipped into the molten alloy was 10 mm. All ingots were cut by 24 mm away from the bottom along the radial direction by molybdenum wire.

Specimens were also ground with SiC abrasive papers, polished and etched by picric acid, which were prepared for solidification structure and precipitate observation conducted by optical microscopy (OM), scanning electron microscopy (SEM) and energy diffraction spectrum (EDS).

### 3 Experimental results and discussion

#### 3.1 Effect of different ultrasonic treatment on structure of Fe-36Ni invar alloy

The macrostructures of Fe-36Ni invar alloy without and with ultrasonic treatment at the same temperature are il-

**Table 2:** Detailed experimental process

G	T (K)	U	Detailed experimental process
G1	1803	N	After adding Si and Al in molten alloy, cast into an ingot mold, air-cooled to room temperature.
G2	1803	B	After adding Si and Al in molten alloy, ultrasonic treatment before solidification, processing time, power and frequency were 45 s, 250 W and 20 KHz respectively. Then, cast into an ingot mold, air-cooled to room temperature.
G3	1803	N	After adding Si and Al in molten alloy, furnace-cooled to room temperature in crucible.
G4	1803	D	After adding Si and Al in molten alloy, ultrasonic treatment until to solidification, processing power and frequency were 250 W and 20 KHz respectively. Then furnace-cooled to room temperature in crucible.
G5	1753	N	After adding Si and Al in molten alloy then added 0.5 g yttrium and kept 1753 K for 180 s, cast into an ingot mold, air-cooled to room temperature.
G6	1753	B	After adding Si and Al in molten alloy then added 0.5 g yttrium and kept 1753 K for 180 s, ultrasonic treatment before solidification, processing time, power and frequency were 60 s, 100 W and 20 KHz respectively. Then, cast into an ingot mold, air-cooled to room temperature.
G7	1803	N	After adding Si and Al in molten alloy then added 0.5 g yttrium and kept 1803 K for 180 s, cast into an ingot mold, air-cooled to room temperature.
G8	1803	B	After adding Si and Al in molten alloy then added 0.5 g yttrium and kept 1803 K for 180 s, ultrasonic treatment before solidification, processing time, power and frequency were 60 s, 100 W and 20 KHz respectively. Then, cast into an ingot mold, air-cooled to room temperature.

*Note:* G = Groups of raw material, T = Test temperature, U = Ultrasonic-treatment methods, N = Without ultrasonic treatment, B = Ultrasonic treatment before solidification, D = Ultrasonic treatment during solidification

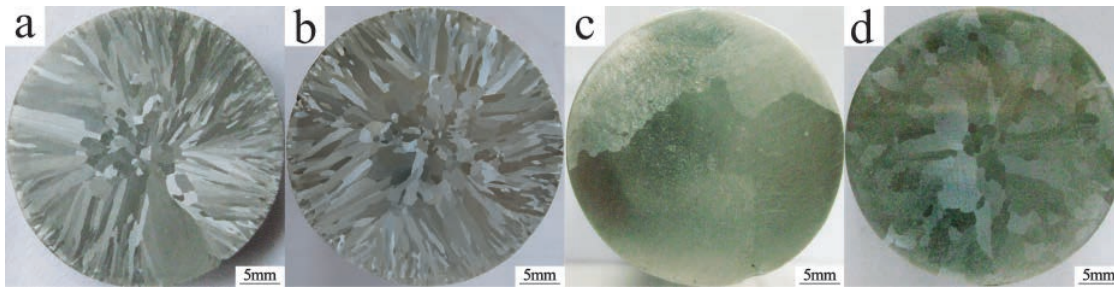


**Fig. 2:** Macrostructures of Fe-36Ni invar alloy: a) G1 without ultrasonic treatment before solidification at 1803 K, b) G2 with ultrasonic treatment before solidification at 1803 K, c) G3 without ultrasonic treatment during solidification at 1803 K, d) G4 with ultrasonic treatment during solidification at 1803 K

illustrated in Fig. 2. And Fig. 2a and b display a certain similarity in terms of the macrostructure. However, Fig. 2c and d show a definite difference in grain numbers. The former only has four big grains while the latter has many grains with small size.

Ultrasonic treatment before solidification had no significant effect on the solidification structure of Fe-36Ni invar alloy. However, when ultrasonic was inputted into the molten alloy during its solidification, the solidification structure was refined significantly. When the ultrasonic probe was dipped into the molten alloy, it could cause a certain degree of super-cooling in a small volume. Therefore, lots of primary dendrites appeared and were broken up into a mass of fragments subsequently. Unfortunately, the temperature of the molten alloy was very high. These fragments were melted and disappeared. Therefore, ultrasonic treatment has no effect on the macrostructure of Fe-36Ni alloy. However, it had an opposite effect when the ultrasonic was inputted into the molten alloy during its solidification. Ultrasonic cavitation could break up the primary and growing dendrites into many small nucleation cores, which survived as the temperature decreased. Under the role of acoustic streaming, these cores were distributed into the whole of the melt uniformly. As a result, the structure of Fe-36Ni alloy was improved significantly.

External ultrasonic treatment applied in molten metal generates a strong nonlinear effect, which causes the cycling alternating positive-negative pressure in local zone of the melt [14]. During the negative period of the cycle, if the negative pressure of ultrasonic is larger than the summation of environment pressure and liquid strength, some small cavitation bubbles appear at the weak regions of melt. Then bubbles expand their sizes many times instantaneously and if the intensity of the positive pressure is high enough, some bubbles collapse

rapidly in the following positive period of the cycle. During bubbles collapsing, the equivalent impulse force is produced in the local zone and can be described as [15]:

$$F_{\text{rad}} = \Gamma_{\text{abs}} \cdot \left( \frac{e_1}{c} \right) \quad (1)$$

where  $F_{\text{rad}}$  is the impulse force,  $\Gamma_{\text{abs}}$  is the local ultrasonic energy absorbed by the material,  $c$  is the speed of ultrasonic in melt and  $e_1$  is a unit vector in the propagation direction of ultrasonic.

The function of ultrasonic attenuation in liquid medium can be defined as [16]:

$$I_t(x) = I_{\text{in}} \cdot \exp(-2\alpha x) \quad (2)$$

where  $I_{\text{in}}$  and  $I_t(x)$  are the incident and target intensities respectively,  $x$  is the transmitted distance and  $\alpha$  is the attenuation coefficient.

Thus, the total ultrasonic energy absorbed by melt is:

$$\Gamma_{\text{abs}} = \int_S I_t(x) dS \quad (3)$$

where  $dS$  is an infinitesimal area on which ultrasonic vibration is imposed.

From Eq. (1), (2) and (3), we have

$$F_{\text{rad}} = I_{\text{in}} \cdot S \cdot \exp(-2\alpha x) \cdot \left( \frac{e_1}{c} \right) \quad (4)$$

According to Eq. (4), it is to be noted that the impulse force is in direct proportion to the incident ultrasonic intensity. When the impulse force is large enough to be able to break up primary and growing dendrites and make the growing crystals vibrate violently, it can cause

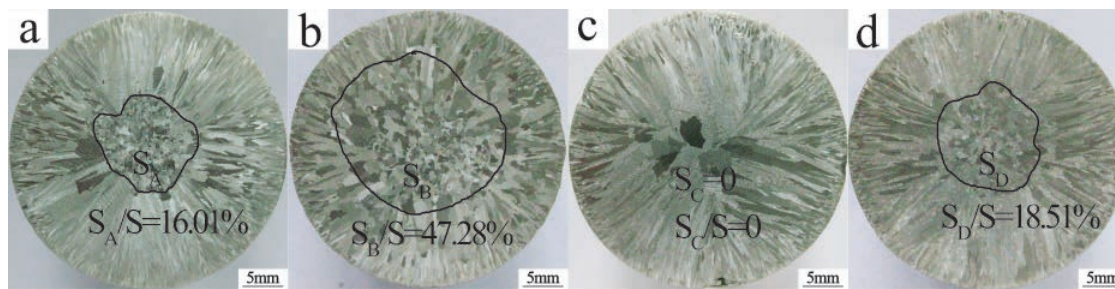


**Fig. 3:** Macrostructures of Fe-36Ni invar alloy doped with yttrium: a) G5 without ultrasonic treatment before solidification at 1753 K, b) G6 with ultrasonic treatment before solidification at 1753 K, c) G7 without ultrasonic treatment before solidification at 1803 K, d) G8 with ultrasonic treatment before solidification at 1803 K

the increasing number of nuclei and their distribution in the whole of the melt uniformly. Therefore, in this experiment, macrostructure is refined significantly under the condition of ultrasonic treatment applied in the molten Fe-36Ni alloy during its solidification.

### 3.2 Effect of ultrasonic treatment on structure of Fe-36Ni invar alloy doped with yttrium

Fig. 3 shows the solidification structure of Fe-36Ni alloy doped with yttrium. Obviously, the conclusion could be drawn that the equiaxed grain zone increased dramatically and solidification structure of Fe-36Ni alloy doped with yttrium were refined significantly when ultrasonic treatment was applied in the melt before its solidification at the same temperature.

Precipitates in the equiaxed grains of the alloy doped with yttrium were tested by scanning electron microscopy (SEM) equipped with energy diffraction spectrum (EDS). A certain number of yttria, yttrium sulfide and yttrium oxy-sulfide could be found. Fig. 4 shows the morphology of precipitates. The precipitate is a spherical particle and its chemical composition is illustrated in Table 3. Yttrium is a

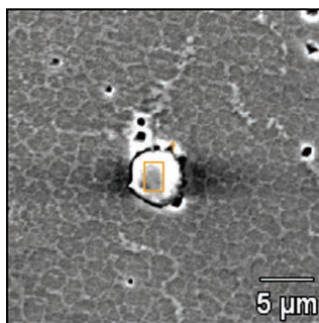


**Fig. 4:** Morphology of precipitate inside the equiaxed grains

**Table 3:** Chemical composition of precipitate inside the equiaxed grains (mass%)

O	Y	Al	Fe	Ni
22.93	58.52	12.75	4.25	1.55

surface-active element. It can form oxide combining with the residual oxygen easily, when it is added in the molten metal. Under some certain conditions, these particles with a high melting point can function as heterogeneous nucleation cores.

On the basis of the disregistry theory of B. L. Bramfitt, etc [17]. Whether the high melting point compound becomes a nucleus for heterogeneous nucleation depends on lattice disregistry between two phases, i.e.:

$$\delta_{(hkl)_s}^{(hkl)_n} = \sum_{i=1}^3 \frac{|d_{[uvw]_s} \cos \theta - d_{[uvw]_n}|}{d_{[uvw]_n}} \times 100\% \quad (5)$$

where  $\delta$  is the disregistry mentioned above,  $(hkl)_s$  is the low index lattice plane of the compound,  $[uvw]_s$  is the low index direction of  $(hkl)_s$ ,  $(hkl)_n$  is the low index lattice plane of the new crystalline phase,  $[uvw]_n$  is the low index direction of  $(hkl)_n$ ,  $d_{[uvw]_n}$  is the lattice plane distance in the direction of  $[uvw]_n$ ,  $d_{[uvw]_s}$  is the lattice plane distance in the direction of  $[uvw]_s$  and  $\theta$  is the angle between  $[uvw]_s$  and  $[uvw]_n$ .

Tables 4 and 5 show the crystallographic data of effective nucleating agents and Fe-36Ni invar alloy and the lattice disregistry between  $Y_2O_3$  and Fe-36Ni invar alloy respectively. The lattice disregistry ( $\delta$ ) between  $Y_2O_3$  and Fe-36Ni is 1.82%. It is lower than 12% (the lowest percentage under which the heterogeneous nucleus could be formed). Therefore,  $Y_2O_3$  is able to act as the heterogeneous nuclei, which is also affected by ultrasonic treatment in molten alloy.



**Table 4:** Crystallographic data of effective nucleating agents and Fe-36Ni invar alloy

Nucleate particle	Crystal type	Lattice parameters/Å(RT)	Lattice parameters/Å(1703 K)
		a	a1
Y <sub>2</sub> O <sub>3</sub>	BCC	10.602	—
Fe-36Ni	FCC	3.64	3.681

$S_A$ ,  $S_B$ ,  $S_C$  and  $S_D$  are the areas of the equiaxed grains (marked in the black line) of specimens while  $S$  is the area of the ingots transverse section, which are measured by Image Tool, as displayed in Fig. 3. And it can also be found that the value of  $S_B$  is larger than  $S_A$ . That is to say, the solidification structure of specimen treated by ultrasonic is better than that untreated by ultrasonic when the treatment temperature is 1753 K. And there is the same regularity when the treatment temperature is 1803 K. Fig. 5 shows large precipitates in specimens treated by ultrasonic are broken up into small ones, which are distributed into the whole of the melt uniformly under the role of acoustic streaming. In samples treated by ultrasonic at 1753 K, the number of the precipitates is 623/mm<sup>2</sup> and its average size is 2.18  $\mu$ m; while untreated by ultrasonic, they are 208/

**Table 6:** Statistics results of precipitates in the samples doped with yttrium

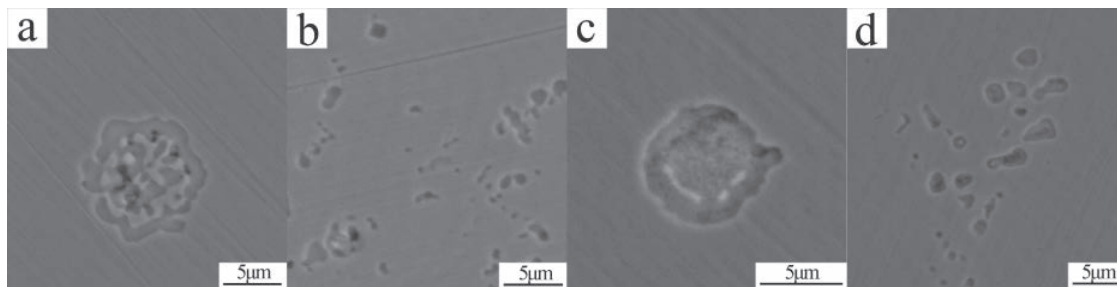
Sample in X group	Number of precipitates per unit area (/mm <sup>2</sup> )	Average size ( $\mu$ m)
G6	623	2.18
G5	208	5.33
G8	604	2.34
G7	178	5.64

mm<sup>2</sup> and 5.33  $\mu$ m respectively. In the same way, there is the same regularity in the specimens treated and untreated by ultrasonic when the treatment temperature is 1803 K, as shown in Table 6.

Thus, it can be concluded that ultrasonic cavitation can break up the precipitates into a great quantity of small particles and acoustic streaming makes them distribute uniformly when ultrasonic treatment is applied in the molten Fe-36Ni alloy doped with yttrium before its solidification [18]. That is to say, it increases the number of nuclei and nucleation probability. Therefore the solidification structure was refined greatly when ultrasonic treatment was applied in the molten alloy doped with yttrium before its solidification.

**Table 5:** Lattice disregistry between Y<sub>2</sub>O<sub>3</sub> and Fe-36Ni invar alloy

$(hkl)_s Y_2O_3 // (hkl)_n Fe-36Ni$	$[uvw]_s$	$[uvw]_n$	$d[uvw]_s$	$d[uvw]_n$	$\theta/(^\circ)$	$\delta/\%$
(100) Y <sub>2</sub> O <sub>3</sub> // (100) Fe-36Ni	[001]	[011]	10.602	10.412	0	1.82
	[011]	[010]	14.993	14.724	0	
	[010]	[01 $\bar{1}$ ]	10.602	10.412	0	
(110) Y <sub>2</sub> O <sub>3</sub> // (110) Fe-36Ni	[001]	$\bar{1}10$	10.602	7.809	0	21.16
	$\bar{1}11$	$\bar{1}12$	14.993	13.524	0	
	$\bar{1}10$	[001]	9.182	11.043	0	
(111) Y <sub>2</sub> O <sub>3</sub> // (111) Fe-36Ni	$\bar{1}01$	[011]	14.993	15.618	0	4.00
	$\bar{2}11$	$\bar{2}11$	25.969	27.048	0	
	$\bar{1}10$	$\bar{1}10$	14.993	15.618	0	

**Fig. 5:** Morphology of precipitates in samples doped with yttrium at two different temperatures: a) G5 without ultrasonic treatment before solidification at 1753 K, b) G6 with ultrasonic treatment before solidification at 1753 K, c) G7 without ultrasonic treatment before solidification at 1803 K, d) G8 with ultrasonic treatment before solidification at 1803 K

### 3.3 Effect of the melt temperature on ultrasonic treatment

In the specimen doped with yttrium, the refining mechanism, in short, can be described as follows: ultrasonic cavitation breaks up the precipitates into lots of small ones, which causes the increasing in the number of nuclei and then refines grains, as shown in the Section 3.2. That is to say, there is a positive correlation between cavitation and the number of nuclei. And it is also easy to know that the value of  $S_B$  is larger than  $S_D$ , as shown in Fig. 3. Therefore, it is inferred that ultrasonic cavitation at 1753 K is better than that at 1803 K. However, the ultrasonic cavitation is much better under a low melt viscosity, which appeared in a melt with a higher temperature [19]. In order to verify the above deduction, the number of precipitates (nucleation cores) is measured, as shown in Table 6. In samples treated by ultrasonic at 1753 K, the number of the precipitates is 623/mm<sup>2</sup> and its average size is 2.18  $\mu\text{m}$ ; while at 1803 K, they are 604/mm<sup>2</sup> and 2.34  $\mu\text{m}$  respectively.

And Fig. 5 shows the morphology of precipitates. Obviously, in specimens with ultrasonic treatment at two different temperatures, large precipitates are broken up into small ones under the condition of ultrasonic cavitation. Meanwhile, the average size is smaller than 5  $\mu\text{m}$  and even the minimum size is less than 0.5  $\mu\text{m}$ .

It can be concluded that the number and size of nucleation cores are almost the same, namely ultrasonic cavitation has a similar effect at two different temperatures. Therefore the structure refined greatly at 1753 K should be caused by some other reasons. After careful comparison, the only distinction in two different temperatures is the pouring temperature. And the superheat of the molten Fe-36Ni alloy is 50 K when it is poured at 1753 K. While at 1803 K, it is 100 K. Additionally, the value of  $S_A$  in specimen untreated by ultrasonic is larger than  $S_C$ , as shown in Fig. 3. Thus, it can be concluded that the solidification structure of the alloy at a low pouring temperature (namely a low superheat) is better than that at a high one when the ultrasonic cavitation has the same effect in the melt. Therefore, it is the low pouring temperature that caused the solidification structure refined at 1753 K.

## 4 Conclusions

1. When ultrasonic treatment was applied in the molten Fe-36Ni alloy without yttrium before its solidification, it had no effect on its solidification.
2. When ultrasonic was inputted in the molten alloy during its solidification, the number of equiaxed

grains increased and the solidification structure was refined significantly.

3. The solidification structure of specimens doped with yttrium was refined dramatically when they were treated by ultrasonic before their solidification.
4. In samples treated by ultrasonic at 1753 K, the number of the precipitates was 623/mm<sup>2</sup> and its average size was 2.18  $\mu\text{m}$ ; while at 1803 K, they were 604/mm<sup>2</sup> and 2.34  $\mu\text{m}$  respectively. The ultrasonic cavitation almost had the same effect at two different temperatures. It was the low pouring temperature that caused the solidification structure refined at 1753 K.

Received: October 28, 2012. Accepted: January 11, 2013.

## References

- [1] Park N J, Oh M H, Kim S M. Effects of Texture on the Etching Property of Fe-36Ni Invar Sheets. *Metals and Materials International*, 2000, 6(1): 51–56.
- [2] Jasthi B K, Arbogast W J, Howard S M. Thermal Expansion Coefficient and Mechanical Properties of Friction Stir Welded Invar (Fe-36Ni). *Journal of Materials Engineering and Performance*, 2009, 18(7): 925–934.
- [3] Zhao Y, Sato Y S, Kokawa H, et al. Microstructure and Properties of Friction Stir Welded High Strength Fe-36wtNi alloy. *Materials Science and Engineering A*, 2011, 528(25): 7768–7773.
- [4] Muzio G, Alippi A, Bettucci A, et al. A Numerical Method for Studying Nonlinear Bubble Oscillations in Acoustic Cavitation. *Ultrasonics*, 1998, 36(1): 553–557.
- [5] Laborde J L, Bouyer C, Caltagirone J P, et al. Acoustic Bubble Cavitation at Low Frequencies. *Ultrasonics*, 1998, 36(1): 589–594.
- [6] Abramov V, Abramov O, Bulgakov V, et al. Solidification of Aluminium Alloys under Ultrasonic Irradiation Using Water-cooled Resonator. *Materials Letters*, 1998, 37(1): 27–34.
- [7] Han Y, Li K, Wang J, et al. Influence of High-intensity Ultrasound on Grain Refining Performance of Al-5Ti-1B Master Alloy on Aluminium. *Materials Science and Engineering A*, 2005, 405(1): 306–312.
- [8] Jian X, Meek T T, Han Q. Refinement of Eutectic Silicon Phase of Aluminum A356 Alloy Using High-intensity Ultrasonic Vibration. *Scripta Materialia*, 2006, 54(5): 893–896.
- [9] Li X, Li T, Li X, et al. Study of Ultrasonic Melt Treatment on the Quality of Horizontal Continuously Cast Al-1% Si alloy. *Ultrasonics Sonochemistry*, 2006, 13(2): 121–125.
- [10] Liu Q, Zhai Q, Qi F, et al. Effects of Power Ultrasonic Treatment on Microstructure and Mechanical Properties of T10 Steel. *Materials letters*, 2007, 61(11): 2422–2425.
- [11] Liu Q M, Zhang Y, Song Y L, et al. Influence of Ultrasonic Vibration on Mechanical Properties and Microstructure of 1Cr18Ni9Ti Stainless Steel. *Materials & Design*, 2007, 28(6): 1949–1952.

- [12] Zhang S, Zhao Y, Cheng X, et al. High-energy Ultrasonic Field Effects on the Microstructure and Mechanical Behaviors of A356 Alloy. *Journal of Alloys and Compounds*, 2009, 470(1): 168–172.
- [13] Puga H, Barbosa J, Costa S, et al. Influence of Indirect Ultrasonic Vibration on the Microstructure and Mechanical Behavior of Al-Si-Cu Alloy. *Materials Science and Engineering A*, 2012.
- [14] Jhang K Y, Kim K C. Evaluation of Material Degradation Using Nonlinear Acoustic Effect. *Ultrasonics*, 1999, 37(1): 39–44.
- [15] Dalecki D, Raeman C H, Child S Z, et al. Effects of Pulsed Ultrasound on the Frog Heart: III. The Radiation Force Mechanism. *Ultrasound in Medicine & Biology*, 1997, 23(2): 275–285.
- [16] Chaparro-Gonzalez J, Mondragon-Sanchez L, Nunez-Alcocer J, et al. Application of an Ultrasound Technique to Control the Modification of Al-Si Alloys. *Materials & Design*, 1995, 16(1): 47–50.
- [17] Bramfitt B L. The Effect of Carbide and Nitride Additions on the Heterogeneous Nucleation Behavior of Liquid Iron. *Metallurgical and Materials Transactions B*, 1970, 1(7): 1987–1995.
- [18] Li J, Chen W Q. Effect of Ultrasonic Melt Treatment on Solidification Structure and Properties of High Carbon Steel. *Foundry*, 2008, 57(10): 1009–1012.
- [19] Knapp R T, Daily J W, Hammitt F G, et al. *Cavitation*. McGraw-Hill New York, 1970.

